Journal of Pharmaceutical Analysis 9 (2019) 274–283

Contents lists available at ScienceDirect

Journal of Pharmaceutical Analysis

journal homepage: www.elsevier.com/locate/jpa

Original Article

Interaction of repaglinide with bovine serum albumin: Spectroscopic and molecular docking approaches

Suma K. Pawar, Seetharamappa Jaldappagari*

Department of Chemistry, Karnatak University, Dharwad 580 003, India

ARTICLE INFO

Article history:
Received 5 October 2018
Received in revised form
12 March 2019
Accepted 13 March 2019
Available online 16 March 2019

Keywords:
BSA-RPG interaction
Spectroscopic investigation
Molecular docking

ABSTRACT

Repaglinide (RPG) regulates the amount of glucose by stimulating the pancreas to release insulin in the blood. In view of its biological importance, we have examined the interaction between RPG and a model protein, bovine serum albumin (BSA) employing various spectroscopic, electrochemical and molecular docking methods. Fluorescence spectra of BSA were recorded in the presence and absence of RPG in phosphate buffer of pH 7.4. Fluorescence intensity of BSA was decreased upon the addition of increased concentrations of RPG, indicating the interaction between RPG and BSA. Stern-Volmer quenching analysis results revealed that RPG quenched the intensity of BSA through dynamic quenching mechanism. This was further confirmed from the time-resolved fluorescence measurements. The binding constant as calculated from the spectroscopic and voltammetric results was observed to be in the order of $10^4\ M^{-1}$ at 298 K, suggesting the moderate binding affinity between RPG and BSA. Competitive experimental results revealed that the primary binding site for RPG on BSA was site II. Absorption and circular dichroism studies indicated the changes in the secondary structure of BSA upon its interaction with RPG. Molecular simulation studies pointed out that RPG was bound to BSA in the hydrophobic pocket of site II.

1. Introduction

Proteins are the building blocks of life which play a vast variety of roles in the cell. These proteins are an integral part of origin, evaluation and metabolism [1]. Plasma proteins comprise three major fractions *viz.*, albumin, globulin and fibrinogen. Albumin is an abundant and important plasma protein, which regulates the osmotic blood pressure. The decrease in the level of serum albumin leads to severe kidney diseases. Albumins from various sources have gained extensive biomedical and industrial applications besides research interest [2]. BSA has 76% structural homology with human serum albumin (HSA) and hence it is being used as a model protein in clinical medicine.

Repaglinide (RPG), chemically known as 2-Ethoxy-4-(2-((3-methyl-1-(2-(1-piperidinyl)phenyl)butyl)amino)-2-oxoethyl)benzoic acid (Fig. 1), is a new carboxy methyl benzoic acid derivative. It belongs to a class of meglitinides and is used to treat type 2 diabetes. It is the first of a new class of oral antidiabetic drug designed to regulate postprandial glucose excursions in type 2 diabetic patients. Although RPG shows some chemical resemblance to other antidiabetic agents, it differs in its mechanism of action and excretion mechanism [3]. RPG lowers the blood glucose levels by blocking ATP-dependent potassium channels in pancreatic β cells, which in turn stimulates insulin secretion [4]. Since the administered RPG is excreted through biliary excretion, it is considered to be an advantage for type 2 diabetic patients with impaired kidney function [5].

Drug-protein binding is an integral part of many other types of intermolecular interactions in a cellular or organ environment [6]. It is known that the pharmacological effect of a drug is dependent on both its pharmacokinetic and pharmacodynamic properties. These properties of a drug can be altered as a result of protein binding since the bound drug is pharmacodynamically inert and only the free (unbound) drug interacts with receptors [7]. Drugs that are highly bound to protein have a lower concentration of free drug. Higher concentration of protein bound drug in the blood stream results in toxic effects. When drugs bind to protein with a lower binding affinity, there will be larger unbound drug fraction. This condition results in poor distribution of the drug to target tissue as the free drug has shorter elimination half-life than the protein bound drug. Hence, studies on drug-protein binding help in improving the efficacy of a drug by controlling the rate of

Peer review under responsibility of Xi'an Jiaotong University.
* Corresponding author.
E-mail address: jseetharam97@gmail.com (S. Jaldappagari).

https://doi.org/10.1016/j.jpha.2019.03.007

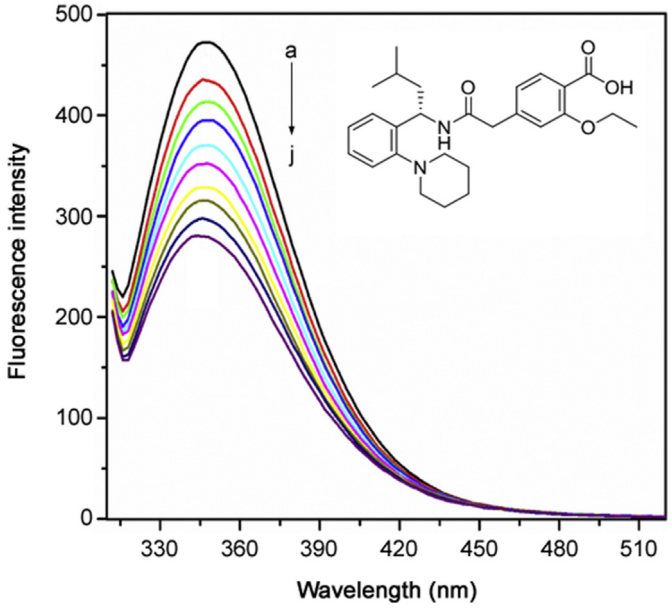

Fig. 1. Effect of increasing concentrations of RPG (b–j) on fluorescence intensity of BSA (a). [BSA] = 1.67 μM, [RPG] (b→j) = 1.67, 3.33, 5.00, 6.67, 8.33, 10.0, 11.7, 13.3 and 15.0 μM.

absorption, distribution, metabolism and excretion of the drug in the body.

For the better therapeutic effects, a drug should reach the targeted site both efficiently and precisely for the necessary period of time. In order to overcome the undesirable properties of drug molecules and drug delivery, cyclodextrins (β-cyclodextrins) are introduced as carrier materials. β-cyclodextrins have been found as potential candidates because of their ability to alter physical, chemical and biological properties of guest molecules through the formation of inclusion complexes [8]. Due to their low toxicity and low immunogenicity, β-cyclodextrins have extremely attractive pharmaceutical applications. They are known to alter various properties of drugs, pharmaceutical formulations, and biomembranes, resulting in enhancement and modulation of rectal drug absorption. Since the cyclodextrin molecule is hydrophilic on the outer surface, the complex formation usually increases the bioavailability of drugs in different administration routes by increasing the solubility, dissolution rate, and wettability of poorly water-soluble drugs and by preventing the degradation or disposition of chemically unstable drugs in gastrointestinal tracts, as well as during storage. Thus, β-cyclodextrin increases the pharmacological effect by allowing a reduction in the dose of the drug administered [9]. This prompted us to investigate the effect of β-cyclodextrin on RPG-BSA interactions.

Seedher and Kanojia have reported the interaction between RPG and HSA by spectroscopic technique [10]. However, they have not carried out the detailed molecular docking and simulation studies on RPG-HSA interactions. Such studies are useful to draw conclusions with regard to binding site for RPG in the protein and stability of docked RPG-protein system. We have discussed these investigations (on RPG-BSA) in the present study. Circular dichroism studies indicated the secondary structural changes in BSA upon interaction with RPG. These studies were not carried out by Seedher and Kanojia. Further, they have not carried out life time measurements, fluorescence resonance energy transfer (FRET) and electrochemical studies. Our electrochemical measurements also supported the results obtained by fluorescence studies (with regard to binding constant and number of binding sites). No report is available in the literature with regard to the interaction of RPG with BSA. In view of the above, we explored the binding characteristics of RPG with BSA by employing multispectroscopic techniques and molecular simulation methods to understand the mechanism of quenching, to determine the binding affinity of RPG towards BSA and to find out the specific binding site and number of binding sites for RPG in BSA besides studying the effect of RPG on secondary structure of BSA. The influence of β-cyclodextrin and metal ions on RPG-BSA binding affinity was also studied.

2. Materials and methods

2.1. Chemicals and reagents

Fatty acid and globulin free BSA, phenylbutazone, ibuprofen and β-cyclodextrin purchased from Sigma Chemical Company (St. Louis, MO, USA) were used without further purification. RPG was obtained as a gift sample from Dr. Reddy's Laboratory, India. A stock solution of BSA (250 μM) was prepared in 0.1 M phosphate buffer of pH 7.4. Phosphate buffer was prepared by mixing suitable amounts of 0.1 M sodium dihydrogen orthophosphate dihydrate and 0.1 M disodium hydrogen orthophosphate dehydrate. Further, an appropriate amount of NaCl was added to maintain an ionic concentration of 0.15 M. Stock solutions of each of 250 μM RPG and β-cyclodextrin were prepared separately in methanol while stock solutions of each of 250 μM phenylbutazone and ibuprofen were prepared in ethanol.

2.2. Fluorescence studies

Agilent Technologies Carry Eclipse fluorescence spectrophotometer equipped with a xenon flash lamp source and a Cary single cell peltier for temperature control was used to perform fluorescence measurements. Both the excitation and emission slit widths were set at 5 nm. Preliminary studies were performed to optimize the experimental parameters. Experimental parameters such as concentration of BSA and RPG, and temperature were optimized and maintained throughout the experiment. BSA was excited at 295 nm and fluorescence spectra were recorded in the presence and absence of RPG in the range of 300–520 nm at 298, 303 and 308 K. For this, the concentration of BSA was fixed at 1.67 μM while that of RPG was varied from 1.67 to 15.0 μM.

2.3. Time-resolved fluorescence lifetime measurements

Fluorescence decay of BSA was recorded on a Chronos BH time-resolved fluorescence lifetime spectrometer 90021 (ISS, USA) in the presence and absence of increasing concentrations of RPG. The excitation and emission wavelength of BSA was fixed at 290 and 344 nm, respectively. The concentration of BSA was fixed at 1.67 μM and that of RPG was varied from 1.67 to 11.7 μM. The goodness of fit was estimated using $\chi 2$ values.

2.4. Displacement studies

Displacement experiments were performed using two different site probes *viz.*, phenylbutazone and ibuprofen for site I and site II, respectively. For this, the concentration of BSA and site probe was kept constant (1.67 μM) while that of RPG was varied from 1.67 to 15.0 μM.

2.5. Fluorescence resonance energy transfer measurements

We have recorded the fluorescence emission spectrum of BSA (1.67 μM) and absorption spectrum of RPG (1.67 μM) separately.

Then, the emission spectrum of BSA was overlapped with absorption spectrum of RPG by plotting double-Y plot in origin software. The values of efficiency of energy transfer (E), overlap integral of emission spectrum of donor and absorption spectrum of acceptor (J) and the critical distance (R_o) were then calculated.

2.6. UV absorption studies

Absorption measurements were carried out on a AU-2701 UV–Vis double beam spectrophotometer (India). Absorption spectra of BSA were recorded at 298 K in the presence and absence of RPG in the wavelength range of 230–380 nm. The concentration of BSA was fixed at 1.67 μM whereas that of RPG was varied from 1.67 to 15.0 μM.

2.7. Circular dichroism (CD) studies

Jasco J-715 spectropolarimeter (Tokyo, Japan) with a cell path length of 1 mm was used for CD measurements. CD spectra of BSA before and after the addition of RPG were recorded in phosphate buffer of pH 7.4 at 298 K in the wavelength range of 200–260 nm. The concentration ratio of BSA to that of RPG was maintained at 1:0, 1:2 and 1:6, respectively.

2.8. Influence of β-cyclodextrin on RPG-BSA binding

For this study, we have recorded fluorescence emission spectra of RPG-BSA system in the presence and absence of β-cyclodextrin in phosphate buffer of pH 7.4 at room temperature. The concentration of RPG was varied from 1.67 to 15.0 μM while that of BSA and β-cyclodextrin was fixed at 1.67 μM.

2.9. Effect of metal ions

Fluorescence emission spectra of RPG-BSA system were recorded at 298 K in the presence and absence of Cu^{2+} and Zn^{2+} ions, separately. For this, the concentration of BSA and metal ion was kept constant (1.67 μM) whereas that of RPG was varied from 1.67 to 15.0 μM [11,12].

2.10. Molecular docking studies

Molecular docking studies were performed using Glide module from Schrodinger software (Schrodinger Release 2014-4: Maestro, version 10.0, Schrodinger, LLC, New York, NY, 2014).

2.10.1. Protein preparation

X-ray crystal structure of BSA (PDB ID-4OR0) was taken from protein data bank (PDB) database (www.rcsb.org/). Before we could proceed for docking process, the protein structure was optimized using protein preparation wizard module (Prepwiz) in Schrodinger. In the first step by preprocess option bond orders were assigned and hydrogens were added. The heteroatoms are ionized by epic at biological pH to consider the protein permeability and drug solubility and then the H-bonds were optimized to reduce the steric clashes by histidine, aspartate, glutamate, and hydroxyl containing amino acids. In the final step by using OPLS3 force field, complete protein structure was minimized to a least possible energy state.

2.10.2. Ligand preparation

In Schrodinger ligprep tool was used where 2D ligand structure was converted into 3D. Further, the ligand structure was optimized by minimizing its energy using OPLS3 force field. The optimized low energy ligand conformations were used for docking studies.

2.10.3. Molecular docking

RPG-BSA docking was performed using glide application. Receptor grid was generated which had a default set of options with van der Waals radius of 1.0 A. These grids were then used to calculate the interaction of prepared ligand with the receptor using the xp ligand docking in glide. The lowest energy conformation with hydrogen bonding was considered further.

2.11. Molecular dynamics simulations

Molecular dynamics simulations were performed using Desmond version 4.4 (Schrödinger Desmond, 2015) module. During simulation, water molecules were simulated by using the water model TIP3P with force filed OPLS3. By using the orthorhombic periodic boundary conditions the boundary regions for the simulations were set and appropriate Na^+ and Cl^- ions were added in the solvated system to electrically neutralize the system. Prior to simulation, ligand-protein complex was formed in the solvated system. This complex was further minimized by protocol of Desmond module using OPLS3 force field. After creation of minimized solvent system, simulations were equilibrated for 10 ns and then molecular dynamic simulations were performed by maintaining the temperature and pressure at 300 K and 1 atmospheric pressure, respectively. The trajectory was stored every 10 ns and further analyzed for calculating the root mean square deviations (RMSD) and root mean square fluctuations (RMSF).

2.12. Electrochemical studies

Voltammograms were recorded on a CHI-1103a Electrochemical Analyser (CH Instruments Ltd. Co.,USA, version 4.01) equipped with a conventional three-electrode system. A glassy carbon electrode (GCE) modified with graphene oxide (GO) was used as the working electrode. A platinum wire and Ag/AgCl electrode was used as counter electrode and reference electrode, respectively. Differential pulse voltammograms (DPV) of RPG were recorded in the absence and presence of BSA in the potential range of 0.2–1.3 V in the Briton Robinson (BR) buffer of pH 7.4. During the experimental process, the concentration of RPG was kept constant (30.61 μM) while that of BSA was varied from 2.55 to 10.2 μM.

3. Results and discussion

3.1. Steady-state fluorescence spectra

Fluorescence spectroscopy is one of the most convenient and successful methods applied to study drug-protein interactions [13]. Fluorescence measurements provide information on drug-protein interaction such as the quenching mechanism, binding affinity between the drug and protein, binding site for the drug on protein, nature of binding force and the intermolecular distance between the drug and protein molecule [14]. Thus, fluorescence measurements of BSA in the absence and presence of different concentrations of RPG were performed to understand the binding characteristics of RPG-BSA interactions. When BSA was excited at 295 nm, it exhibited a strong emission peak at 346 nm (Fig. 1) under physiological conditions. Upon successful addition of RPG, significant quenching in the emission intensity of BSA accompanied by a slight blue shift in the emission wavelength was noticed. The blue shift was attributed to the decreased polarity in the hydrophobic cavity of tryptophan upon binding to RPG. This decreased hydrophobicity resulted in microenvironmental changes around tryptophan residues [15,16].

Absorption of the quencher at the emission and excitation wavelength of fluorophore results in inner-filter effect. So, in order

to minimize this effect, fluorescence intensity of BSA was corrected using the following formula:

$$F_{corr} = F_{obs} \cdot antilog[(A_{ex} + A_{em})]/2 \quad (1)$$

where F_{corr} and F_{obs} are the corrected and observed emission intensities respectively. A_{ex} and A_{em} are the absorbance values of the system at excitation and emission wavelengths, respectively. In this study all the fluorescence intensities mentioned correspond to the corrected fluorescence intensities [17].

To elucidate the mechanism of quenching of BSA by RPG, we performed fluorescence measurements of free BSA and RPG-BSA at 298, 303 and 308 K and the results were examined using the Stern-Volmer equation shown below:

$$F_0/F = 1 + K_q\tau_0[Q] = 1 + K_{sv}[Q] \quad (2)$$

where F_o and F are the fluorescence intensities in the absence and presence of the quencher, K_q is the bimolecular quenching rate constant, τ_o is the average lifetime of the fluorophore in the absence of the quencher, [Q] is the concentration of the quencher and K_{sv} is the Stern-Volmer quenching constant.

Fig. 2 illustrates the Stern-Volmer plots for RPG-BSA complex at 298, 303 and 308 K. From slopes of these plots, the values of K_{sv} were determined and are tabulated in Table 1. The Stern-Volmer plot (F_o/F vs. [Q]) for RPG-BSA interaction (for different temperatures) was found to be linear, indicating the existence of only one type of quenching mechanism. Hence, we ruled out the possibility of combined quenching mechanism. Increased K_{sv} values were observed due to increased number of collisions between RPG and BSA molecules at higher temperatures. This suggested that RPG quenched the intrinsic intensity of BSA through dynamic quenching mechanism [18]. Further, to verify the quenching mechanism, we have performed time-resolved fluorescence spectroscopic studies as it is sensitive to excited state interactions.

3.2. Time-resolved fluorescence spectroscopic studies

Time-resolved fluorescence spectroscopic technique is widely used to distinguish between dynamic and static quenching mechanism. The distinction between two mechanisms is done on the basis of the fact that in dynamic quenching process the average life time of protein (fluorophore) decreases upon interaction with a drug (quencher) whereas in static quenching process, the formation of a nonfluorescent complex does not exhibit any effect on the average life time of uncomplexed fluorophore [19]. Time-resolved fluorescence spectra of native BSA before and after the addition of RPG were recorded upon the excitation of BSA at 290 nm at room temperature. Fig. 3 shows the effect of RPG on decay profile of native BSA. The results obtained were analyzed by tail fitting method with $\chi 2$ values close to unity. The decay profiles of BSA were fitted with bi-exponential function [20]. For bi-exponential function decay curve, the average life time of BSA in the presence and absence of RPG was calculated using the equation shown below [21]:

$$\langle\tau\rangle = (\alpha_1\tau_1 + \alpha_2\tau_2)/(\alpha_1 + \alpha_2) \quad (3)$$

where τ_1 and τ_2 are the decay times and α_1 and α_2 are the pre-exponential factors. The calculated values are summarized in Table 2. The average life time of free BSA was found to be 5.45 ns which decreased to 2.03 ns in the presence of increasing concentrations of RPG. This decrease in the average life time of BSA implied the existence of dynamic quenching mechanism between RPG and BSA interaction.

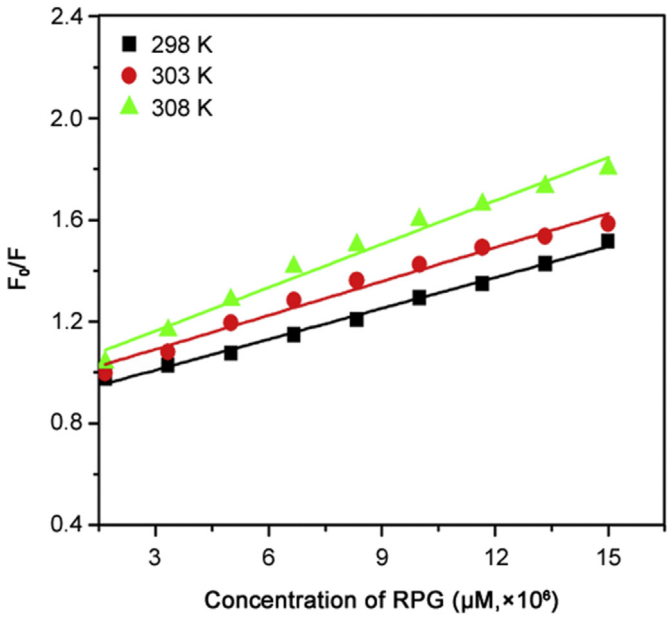

Fig. 2. Stern-Volmer curves for the binding of RPG to BSA at 298, 303 and 308 K, in phosphate buffer of pH 7.4.

3.3. Determination of binding constants and binding sites

Drugs bind reversibly to a protein with different binding affinities. The strength of the drug-protein interaction is measured in terms of their binding affinity. This binding affinity between a drug and protein can be expressed in terms of binding constant (K) [22]. When a drug molecule binds to a set of equivalent sites on a protein, the binding constant and the number of binding sites (n) per protein molecule for a drug-protein system can be calculated using the following equation [23]:

$$\log[(F_0 - F)/F] = \log K + n \log[Q] \quad (4)$$

where K is the binding constant of the system and n is the number of binding sites. The values of K and n for RPG-BSA system at 298, 303 and 308 K were determined from the intercept and slope of log [(F_0–F)/F] vs. log[Q] plot and the results are tabulated in Table 1. It is evident that the binding constant of RPG-BSA increased with an increase in temperature, indicating the increased stability of the system at higher temperatures. The binding constant of RPG-HSA of the order of $10^5\,M^{-1}$ [10] revealed the stronger binding while a moderate binding affinity between RPG and BSA as evident from its binding constant of the order of $10^4\,M^{-1}$. This observation suggested that RPG showed stronger binding affinity for HSA rather than for BSA. The value of n close to 1 revealed that there was only one binding site for RPG per BSA molecule [24].

3.4. Nature of binding force

Various non-covalent interactions act as driving forces in drug-protein interactions. These are electrostatic interactions, van der Waals interactions, hydrophobic forces and hydrogen bond formation [25]. The forces acting between a drug and protein can be determined with the aid of thermodynamic parameters *viz.*, free energy change (ΔG°), entropy change (ΔS°) and enthalpy change (ΔH°). Based on signs and magnitudes of these parameters, Ross and Subramanian have classified nature of acting forces on three possibilities [26].

Table 1
Stern-Volmer quenching constants (K_{sv}), binding constants (K), the number of binding sites (n) and thermodynamic parameters for RPG-BSA system at different temperatures.

T (K)	K_{sv} (L/mol/s)	K (M^{-1})	n	R^2	ΔH^o (kJ/mol)	ΔS^o (J/K/mol)	ΔG^o (kJ/mol)
298	$(4.04 \pm 0.05) \times 10^4$	$(2.76 \pm 0.04) \times 10^4$	1.01	0.98	123.7 ± 2.12	500.5 ± 6.95	-25.3 ± 0.41
303	$(4.45 \pm 0.08) \times 10^4$	$(7.51 \pm 0.12) \times 10^4$	1.05	0.99			-28.2 ± 0.49
308	$(5.68 \pm 0.12) \times 10^4$	$(1.39 \pm 0.02) \times 10^5$	1.04	0.98			-30.3 ± 0.52

R^2 = Correlation coefficient.

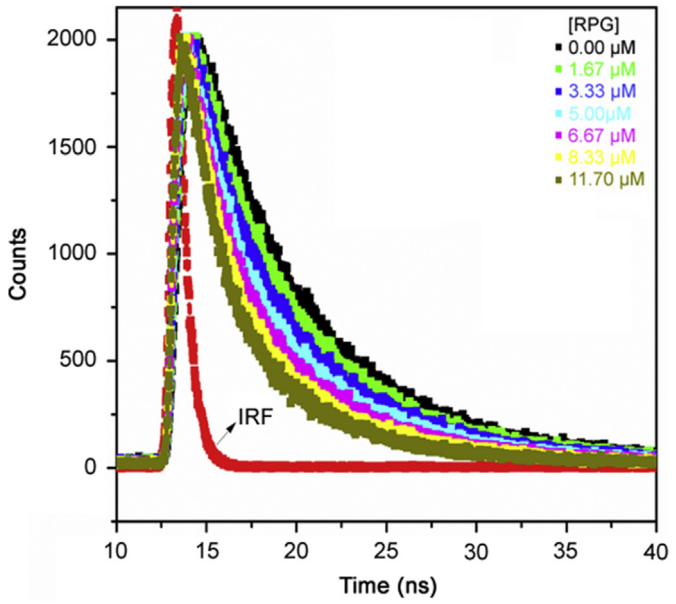

Fig. 3. Time-resolved fluorescence decay profile of BSA in the presence of different concentrations of RPG. [BSA] = 1.67 µM, [RPG] = 1.67–11.7 µM (IRF: Instrument Response).

Table 2
Fluorescence lifetime decay of BSA in the presence of different concentrations of RPG.

System	τ_1	τ_1	α_1	α_2	<J> ns
BSA only	1.83	6.23	3.25	15.1	5.45
RPG[a]					
1.67	1.5	6.16	6.64	14.6	4.70
3.33	1.07	5.92	10.9	14.9	3.87
5.00	0.957	5.72	16	14.8	3.24
6.67	0.899	5.59	21.7	14.4	2.77
8.33	0.834	5.34	27.6	14.4	2.37
11.7	0.754	5.03	34.2	14.7	2.03

[a] Concentration of RPG is in µM.

i) Positive values of ΔS° and ΔH° indicate the presence of hydrophobic forces,
ii) Negative values of ΔS° and ΔH° refer to the existence of hydrogen bonding and/or van der Waals forces,
iii) Negative value of ΔH° and a positive value of ΔS° suggest the contribution of electrostatic forces.

In order to find out the driving force acting between RPG and BSA, we have determined the values of ΔS°, ΔH° and ΔG° for RPG-BSA system using the following van't Hoff and Gibbs free energy equation respectively.

$$\log K = -\Delta H^\circ / 2.303RT + \Delta S^\circ / 2.303R \quad (5)$$

$$\Delta G^\circ = -2.303RT \log K \quad (6)$$

where R is the gas constant and T is the absolute temperature. The values of ΔH° and ΔS° were obtained from the slope and intercept of the van Hoff plot respectively. The values of ΔG° at different temperatures were calculated and are given in Table 1. These negative values of ΔG° revealed the spontaneity of the interaction between RPG and BSA. Positive values of ΔH° and ΔS° suggested the contribution of hydrophobic forces in RPG-BSA binding [27].

3.5. Site markers competitive binding

Crystal structure studies revealed that BSA possesses two principle binding sites *viz.*, site I and site II. Site I and site II are situated in hydrophobic cavities of subdomain IIA and subdomain IIIA, respectively. Site I is relatively larger in size where the most neutral, bulky and heterocyclic compounds tend to bind through hydrophobic interactions. In contrast to this, site II is smaller in size which involves a combination of hydrophobic, hydrogen bonding and electrostatic interactions [28]. In order to determine whether RPG binds to BSA at site I or site II, we have carried out site probe displacement studies. For this two recognized site probes *viz.*, phenylbutazone and ibuprofen which are known to bind BSA at site I and site II, respectively, were selected. Fluorescence spectra of an equimolar mixture of BSA and site probe in the presence of increasing amounts of RPG were recorded at 298 K. Using equation (4), binding constant of RPG-BSA system in the presence and absence of site probes was calculated. The binding constant of RPG-BSA system was remarkably decreased from $(2.76 \pm 0.04) \times 10^4\ M^{-1}$ to $(3.41 \pm 0.04) \times 10^3\ M^{-1}$ in the presence of ibuprofen while it remained almost the same in the presence of phenylbutazone $(2.64 \pm 0.05) \times 10^4\ M^{-1}$. These results suggested that both RPG and ibuprofen competed for BSA at site II, thereby decreasing the binding constant. Based on these observations, we proposed that RPG was bound to BSA at site II of subdomain IIIA.

3.6. Fluorescence resonance energy transfer (FRET)

FRET involves the distance dependent energy transfer from a donor (fluorophore) molecule to an acceptor (quencher) molecule. In FRET, exchange of excitation energy of electronic states takes place from donor to acceptor molecule via a dipole-dipole coupling mechanism [29]. Fig. 4 shows the spectral overlap of absorption spectrum of RPG with emission spectrum of BSA. The values of J, E and R_o for RPG-BSA were calculated to be $0.2906 \times 10^{-15}\ cm^3\ L\ mol^{-1}$, 0.1248 and 1.01 nm, respectively. The distance between BSA and RPG was noticed to be 1.48 nm, which satisfied the condition of $0.5R_o < r < 1.5R_o$ for non-radiant energy transfer between BSA and RPG. This resulted in quenching of fluorescence intensity of BSA [25].

3.7. RPG-induced conformational changes in BSA

3.7.1. UV–vis absorption spectra

To investigate the effect of RPG binding on secondary structure

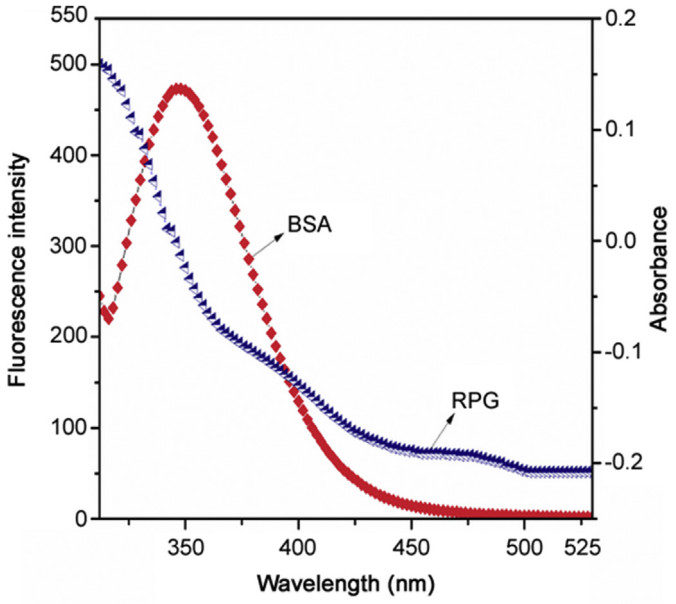

Fig. 4. Spectral overlap between fluorescence emission spectrum of BSA and absorption spectrum of RPG. [BSA] = [RPG] = 1.67 μM.

of BSA, absorption spectra of BSA were recorded in the presence of increasing concentrations of RPG (Fig. 5). Native BSA exhibited a characteristic absorption band at 280 nm which resulted from $\pi \rightarrow \pi^*$ transition of the amino acid residues (Trp, Tyr and Phe) [30]. The absorbance of Trp and Tyr residues depends on the microenvironment of their chromophores, and their shift to either side of wavelength range (i.e. red or blue shift) depends upon the polarity of surrounding environment [31]. Upon successive addition of RPG, significant enhancement in the absorbance of BSA accompanied by a slight red shift in the wavelength maxima was noticed. Peptide strands of the protein were extended more due to increased polarity around the protein residue, resulting changes in the secondary structure of BSA [32–34].

3.7.2. Circular dichroism (CD) studies

In biological chemistry and structural biology, CD technique has been widely used for secondary structure determination [35]. CD spectral studies provide information on the secondary structural element of the protein such as α-helicity and also on conformational alterations in the protein associated with the drug binding [36]. CD spectra were recorded in the range of 200–260 nm (Fig. 6). As displayed in Fig. 6, CD spectrum of BSA exhibited two negative bands in the UV region near 208 and 222 nm, due to π-π^* and n-π^* transitions of the peptide bond, respectively. These two bands signify the α-helicity of the protein [37]. With the addition of RPG, we observed a gradual increase in the intensity of CD bands without imposing any significant shift in the peak positions. This increased band intensity indicated the decreased disordered structural content in the native BSA. Further, it revealed that RPG penetrated into BSA and induced modification in the secondary structural content of BSA [38–40].

3.8. Role of β-cyclodextrin and metal ions on RPG-BSA binding

3.8.1. Effect of β-cyclodextrin on the binding affinity of RPG with BSA

Cyclodextrins can form molecular inclusion complexes with many drugs by incorporating the drug molecule into the central cavity. This increases the aqueous solubility of poorly soluble hydrophobic drugs there by increasing their bioavailability and stability [41,42]. Because of this property, cyclodextrins are used as molecular cages in pharmaceutical, agrochemical, food and cosmetic industries. By considering the role of cyclodextrins in drug delivery, we investigated the effect of β-cyclodextrin on the binding affinity of RPG towards BSA. For this study, we recorded fluorescence spectra of RPG-BSA system in the presence and absence of β-cyclodextrin. The binding constant of RPG-BSA system before and after the addition of β-cyclodextrin was calculated using equation (4). The binding constant of RPG-BSA system decreased from $(4.77 \pm 0.09) \times 10^4\ M^{-1}$ to $(4.48 \pm 0.07) \times 10^3\ M^{-1}$ in the presence of β-cyclodextrin. These results indicated the encapsulation of RPG by β-cyclodextrin that blocked the direct collision of RPG with BSA,

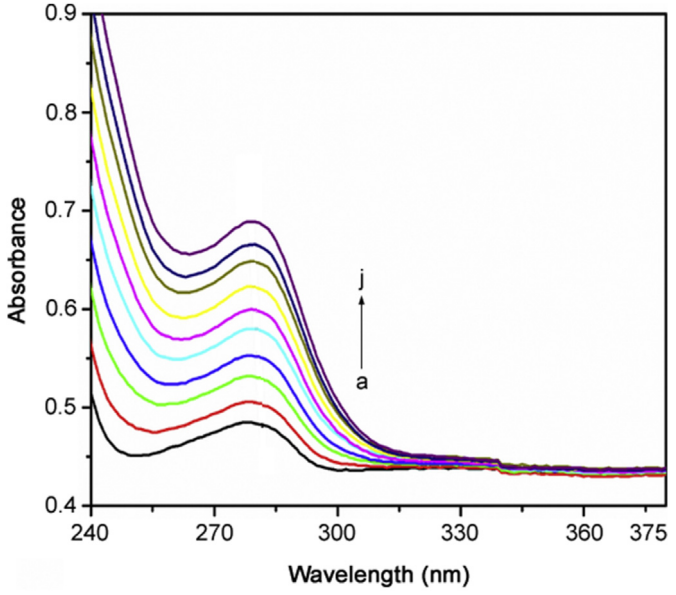

Fig. 5. Absorption spectra of BSA (a) with increasing concentrations of RPG (b–j). [BSA] = 1.67 μM, [RPG] (b → j) = 1.67, 3.33, 5.00, 6.67, 8.33, 10.0, 11.7, 13.3 and 15.0 μM.

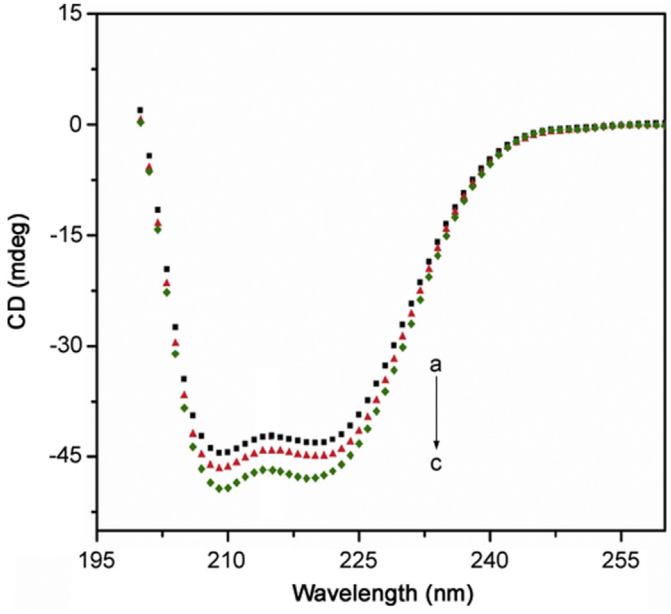

Fig. 6. Circular dichroism spectra of native BSA (1.67 μM) (a) in the presence of RPG; BSA/RPG molar ratio of 1:2 (b) and 1:6 (c).

thereby decreasing the binding affinity between RPG and BSA [43,44]. Further, it suggests that β-cyclodextrin helps in the controlled release of RPG. So, more amount of RPG is freely released which is available to the targeted tissues as compared to RPG released from plasma. This facilitates the RPG to deliver its optimum medicinal effects [12,45].

3.8.2. *Influence of metal ions on RPG-BSA interaction*

Metal ions are imperative components of the cellular machinery and are involved in numerous essential tasks in the biochemical processes [46]. These metal ions interact with protein as well as with drugs in the blood plasma and so the presence of these metal ions may have a significant effect on drug-protein interactions. The increase or decrease in the binding affinity of drug-protein complex in the presence of these metal ions depends on the relative affinity of protein and drug towards the metal ions. So in order to investigate the influence of essential metal ions *viz.,* Cu(II) and Zn(II) on RPG-BSA interaction, fluorescence measurements were performed. For this, fluorescence spectra of an equimolar mixture of BSA and Cu(II)/Zn(II) were recorded with increasing concentrations of RPG and the corresponding binding constants were determined using equation (4). The binding constant of RPG-BSA system was found to be increased from $(2.76 \pm 0.04) \times 10^4\ M^{-1}$ to $(8.95 \pm 0.12) \times 10^4\ M^{-1}$ in the presence of Cu (II), while it decreased to $(2.49 \pm 0.04) \times 10^3\ M^{-1}$ in the presence of Zn(II). Due to higher binding affinity of Cu(II) towards both BSA and RPG, it formed a BSA-Cu(II)-RPG ternary complex where RPG interacted with BSA through metal ion bridge formed by Cu(II). This increased the binding constant between BSA and RPG. The decreased binding constant of RPG-BSA system in the presence of Zn(II) suggested that Zn(II) interacted with BSA and formed a BSA-Zn(II) complex, thereby decreasing the binding constant. The higher binding constant of drug-protein complex in the presence of a metal ion results in the prolonged storage time of the drug in the blood plasma, thereby decreasing the free drug concentration in the body. In contrast to this, the lower binding constant of drug-protein complex results in the increased free drug concentration in the blood plasma which could in turn result in the quick clearance of the drug. Hence, the results of the study will help in altering the doses of RPG in the presence of these metal ions to achieve the desired therapeutic effect [47,48].

3.9. *Molecular docking studies*

From the results of site probe competitive experiments, we proposed that RPG was bound to BSA at site II of subdomain IIIA. To validate this, we performed molecular docking using Schrodinger software. Crystal structure studies revealed that BSA possesses three homologues domains *viz.,* domain I (1–195), domain II (196–383) and domain III (384–583) where each domain contains two subdomains (A and B). Subdomains IIA and IIIA are considered as the main binding sites, site I and site II respectively to which the small molecules bind [49]. The analysis of docked conformations clearly indicated that RPG was bound to BSA in the hydrophobic pocket of site II (Fig. 7A). Stacked bar charts representing RPG-BSA contacts *viz.,* hydrogen bonds, hydrophobic, ionic and water bridges over the course of 10 ns trajectory are shown in Fig. 7B. It is obvious from the figure that amino acid residue Asn-390 formed hydrogen bond with RPG. A value of 0.75 interaction fraction suggested that 75% of the simulation time the specific interaction was maintained. Fig. 7C illustrates the hydrogen bond formation between RPG and amino acid residue of BSA. The amide oxygen (O17) of RPG formed a hydrogen bond with Asn-390 in BSA with a bond distance of 1.84 Å. RPG was surrounded by a number of hydrophobic amino acid residues (Fig. 7D) *viz.,* Gln-389, Leu-386, Asn-385, Ala-489, Ser-488,

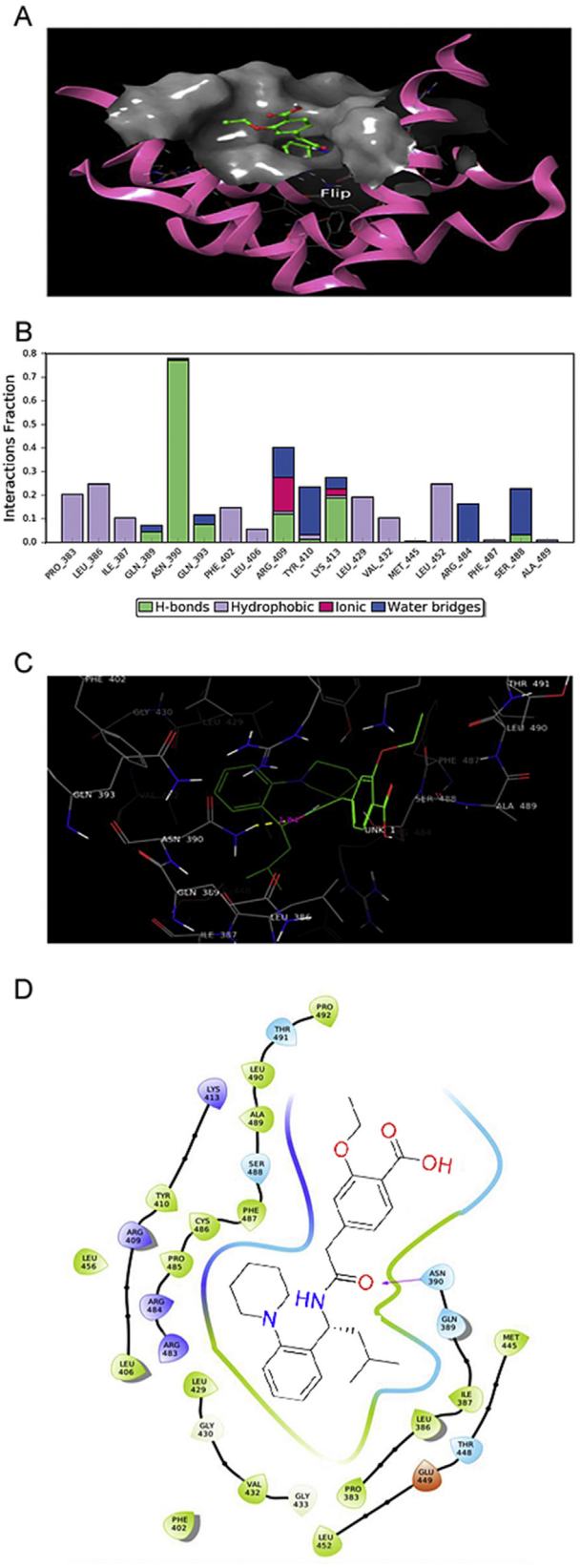

Fig. 7. (A) RPG embedded in the hydrophobic pocket of BSA (site II), (B) RPG-BSA contacts represented by normalized stacked bar charts over the course of 10 ns trajectory, (C) hydrogen bond formation between BSA (Asn-390) and RPG (amide oxygen-O17) and (D) amino acid residues involved in BSA-RPG binding at site II of subdomain IIIA. The purple arrow displayed the hydrogen bonding interaction with Asn-390.

Leu-490, Thr 491, Phe-487, Gln-393, Pro-383, Lys-413, Pro-492, Arg-409, Leu-406, Phe-402, Val-408, Met-445, Thr-448, Glu-449, Gly-433, Val-432, Arg-483, Pro-485 and Ser-488, which shaped the hydrophobic cavity around RPG where it interacted with BSA (Asn-390). The participation of these hydrophobic residues in the RPG-BSA interaction suggested that hydrophobic forces are the main driving forces behind the interaction between RPG and BSA [50]. These results are consistent with the site probe competitive experiments and thermodynamic analysis.

3.10. Molecular dynamics simulation

From the docking studies we proposed the site II as the binding site for RPG on BSA. In order to analyze the stability of the docked RPG-BSA complex, we performed molecular simulation studies using Desmond. The docked conformation of RPG-BSA system was subjected to simulation process for 0–10 ns. When both BSA and RPG are allowed to move freely under explicit salvation, the stability, rigidity and microenvironmental changes for RPG-BSA complex can be explained on the parameters like RMSD and RMSF. The plot for the RMSD values of the protein backbone in pure BSA and RPG-BSA complex as a function of time (0–10 ns) are shown in Fig. 8A. RPG-BSA complex was first aligned on BSA backbone and the corresponding RMSD values were measured. Initially, both the systems reached equilibration and at the same time the RMSD values of BSA and RPG-BSA were increased to 2.6 Å till 2 ns of simulation time. In 2–4 ns, RPG-BSA complex diffused away from BSA, resulting in a decreased RMSD value from 2.6 Å to 1.6 Å. Then, RMSD value of RPG-BSA complex increased to 2.8 Å and then oscillated nearly 5.8 ns. Later, the RMSD value of RPG-BSA complex fluctuated more from 5.8 to 8.2 ns of simulation time. After 8 ns again both the systems equilibrated and attained stability by conformational rearrangement till the end of the simulation (10 ns). The local changes in the amino acid residues of BSA in RPG-BSA complex during simulation were assessed by finding the RMSF values. RMSF of BSA in RPG-BSA complex was plotted as a function of residue number, and the plot shows the fluctuation of total amino acids of total polypeptide chain (Fig. 8B). In the RMSF plot, the observed peaks indicate the areas of protein that fluctuate the most during simulation [51]. As evident from the figure, fluctuations in the subdomain IIIA (380–480 amino acid residues) were found to be less than other subdomains (IA, IB, IIA, IIB, and IIIB). This clearly suggested that RPG was bound to BSA in the subdomain IIIA and formed a rigid structure during MD simulation [52].

3.11. Electrochemical characterization of RPG-BSA interaction

Interaction between a small molecule and serum protein by voltammetric techniques can be investigated by monitoring the difference in the redox peak current and peak potential of the characteristic system before and after the addition of macromolecule [53]. Differential pulse voltammograms of RPG in the presence and absence of BSA are shown in Fig. 9. RPG exhibited an irreversible oxidation peak at 0.83 V in BR buffer of pH 7.4. The peak current of RPG was gradually decreased with the successive addition of BSA and a slight negative shift in the peak potential was noticed. This observation indicated that the interaction of RPG with BSA resulted in the formation of a non-electrochemically active RPG-BSA complex at the electrode surface. The non-electrochemical active compound decreased the concentration of free RPG and eventually decreased the oxidation peak current [54].

By assuming that the interaction of RPG with BSA yields a single BSA-mRPG complex, the binding constant (β) and binding ratio (m) for the single complex can be calculated using the following equation [55]:

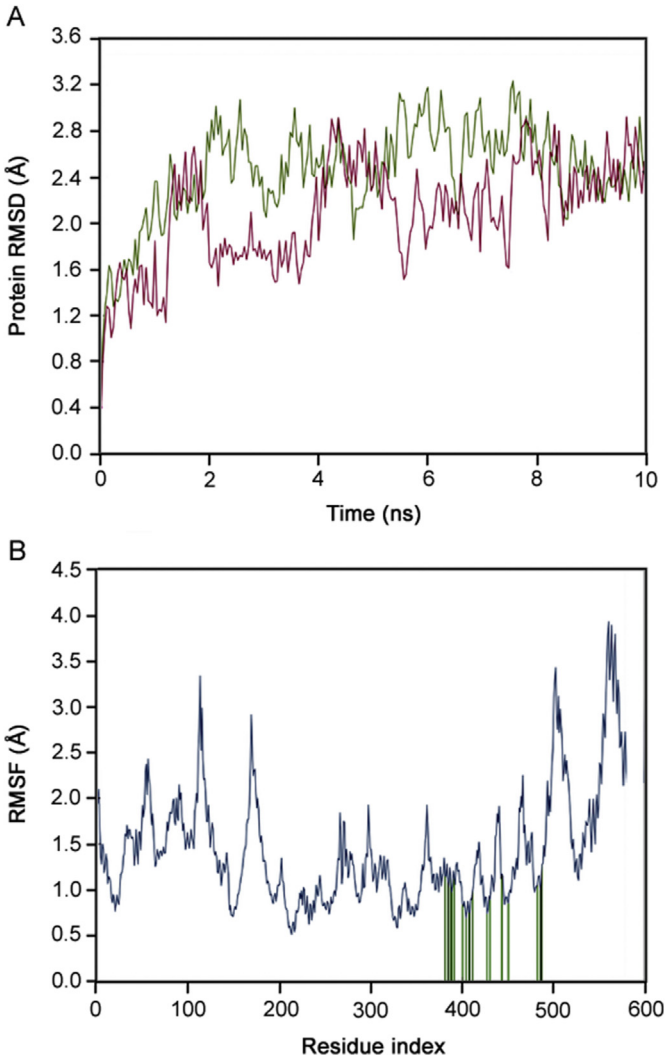

Fig. 8. (A) RMSD plot, green colour represents RMSD of BSA while red colour represents that of RPG-BSA complex and (B) RMSF plot, blue peaks indicate areas of the protein that fluctuate the most during simulation and green colour vertical bars represent the BSA residues that interact with RPG.

$$\log[\Delta I/\Delta I^{\circ}_{max} - \Delta I] = \log \beta + m \log [Q] \quad (7)$$

where ΔI is the difference in peak current of RPG in the presence and absence of BSA, ΔI_{max} is the maximal change in the peak current when the concentration of RPG is extremely higher than that of BSA and *[Q]* is the concentration of RPG. From the slope and intercept of the plot of log $[\Delta I/\Delta I_{max} - \Delta I]$ versus log *[Q]*, the values of m and β were calculated and are found to be 1.1 and $(1.77 \pm 0.03) \times 10^4\ M^{-1}$ at room temperature, respectively. The value of *m* indicates that there is 1:1 binding stoichiometry for RPG-BSA interaction, which in turn suggests that BSA has only one binding site for RPG [56]. The value of binding constant obtained from voltammetric studies is in good agreement with that obtained from spectroscopic results.

4. Conclusions

The present work provides various methodologies to understand the mechanism of interaction of pharmaceutically important drug, RPG with BSA. Fluorescence spectroscopic measurements

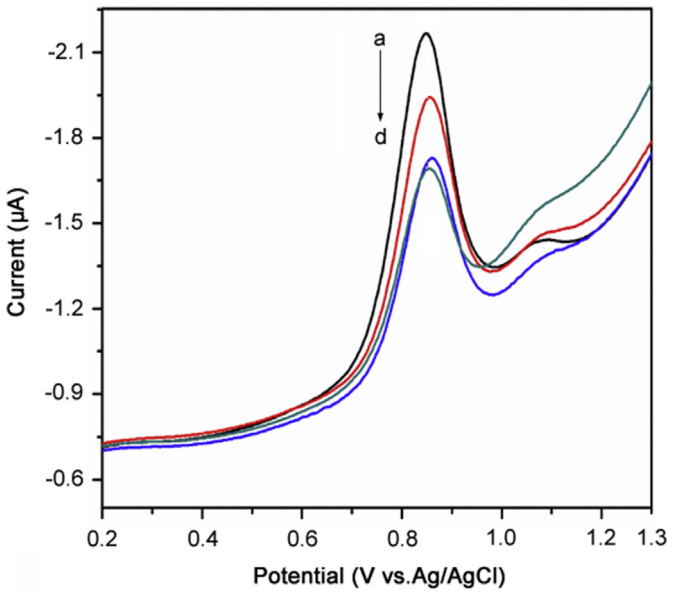

Fig. 9. Differential pulse voltammograms of RPG in the absence (a) and presence of BSA (b→d). [RPG] = 30.61 μM, [BSA] (b→d)= 2.55–10.2 μM.

confirmed that RPG interacted with BSA and quenched its fluorescence intensity via dynamic quenching mechanism. This was supported by time-resolved fluorescence lifetime measurement studies. The location of binding site for RPG in BSA was investigated by site probe displacement experiments and molecular docking studies, and the results indicated that RPG was bound to BSA at site II. Thermodynamic studies revealed that the hydrophobic interactions played a pivotal role in RPG-BSA interaction. The change in secondary conformation of BSA upon interaction with RPG was explored by absorption and CD studies.

Acknowledgments

The authors thank the University Grants Commission, New Delhi, for providing the financial support to carry out this work [F.No 43-205/2014(SR) dated 18-08-2015]. Thanks are owe to the Chairman, Department of Molecular Biophysics, Indian Institute of Science, Bangalore, for CD facilities. One of the authors (Suma K. Pawar) acknowledges the University Grants Commission, New Delhi, for awarding the Rajiv Gandhi National Fellowship (F1-17.1/2016-17/RGNF-2015-17-SC-KAR-11858 dated January 2016).

Conflicts of interest

The authors declare that there are no conflicts of interest.

Appendix A. Supplementary data

Supplementary data to this article can be found online at https://doi.org/10.1016/j.jpha.2019.03.007.

References

[1] P. Bolel, N. Mahapatra, M. Halder, Optical spectroscopic exploration of binding of Cochineal Red A with two homologous serum albumins, J. Agric. Food Chem. 60 (2012) 3727–3734.
[2] B.X. Huang, H.Y. Kim, C. Dass, Probing three-dimensional structure of bovine serum albumin by chemical cross-linking and mass spectrometry, J. Am. Soc. Mass Spectrom. 15 (2004) 1237–1247.
[3] M.A. El-Ries, G.G. Mohamed, A.K. Attia, Electrochemical determination of the antidiabetic drug repaglinide, Yakugaku Zasshi 128 (2008) 171–177.
[4] M. Whirl-Carrillo, E.M. McDonagh, J.M. Hebert, et al., Pharmacogenomics knowledge for personalized medicine, Clin. Pharmacol. Ther. 92 (2012) 414–417.
[5] J. Zhang, F. Gao, X. Guan, et al., Determination of repaglinide in human plasma by high-performance liquid chromatography–tandem mass spectrometry, Acta Pharm. Sin. B 1 (2011) 40–45.
[6] J. Oravcová, B. Böhs, W. Lindner, Drug-protein binding studies new trends in analytical and experimental methodology, J. Chromatogr. B Biomed. Appl. 677 (1996) 1–28.
[7] S. Schmidt, D. Gonzalez, H. Derendorf, Significance of protein binding in pharmacokinetics and pharmacodynamics, J. Pharm. Sci. 99 (2010) 1107–1122.
[8] G. Tiwari, R. Tiwari, A.K. Rai, Cyclodextrins in delivery systems: Applications, J. Pharm. BioAllied Sci. 2 (2010) 72–79.
[9] E.M. Martin Del Valle, Cyclodextrins and their uses: a review, Process Biochem. 39 (2004) 1033–1046.
[10] N. Seedher, M. Kanojia, Reversible binding of antidiabetic drugs, repaglinide and gliclazide, with human serum albumin, Chem. Biol. Drug Des. 72 (2008) 290–296.
[11] Y. Rahman, S. Afrin, M. Tabish, Interaction of pirenzepine with bovine serum albumin and effect of β-cyclodextrin on binding: a biophysical and molecular docking approach, Arch. Biochem. Biophys. 652 (2018) 27–37.
[12] C.Z. Lin, M. Hu, A.Z. Wu, et al., Investigation on the differences of four flavonoids with similar structure binding to human serum albumin, J. Pharm. Anal. 4 (2014) 392–398.
[13] G. Mocz, J.A. Ross, Fluorescence techniques in analysis of protein-ligand interactions, Methods Mol. Biol. 1008 (2013) 169–210.
[14] M.A. Rashid, S.N.I. Rabbi, T. Sultana, et al., Fluorescence spectroscopic study of interaction between olanzapine and bovine serum albumin, Pharm. Anal. Acta 6 (2015) 408.
[15] J.R. Lakowicz, Principles of Fluorescence Spectroscopy, third ed., 2006. New York.
[16] X. Pan, P. Qin, R. Liu, et al., Characterizing the interaction between tartrazine and two serum albumins by a hybrid spectroscopic approach, J. Agric. Food Chem. 59 (2011) 6650–6656.
[17] C.R. Camargo, Í.P. Caruso, S.J.C. Gutierrez, et al., Spectral and computational features of the binding between riparins and human serum albumin, Spectrochim. Acta A Mol. Biomol. Spectrosc. 190 (2018) 81–88.
[18] T.L. Pragna, M. Mondal, K. Ramadas, et al., Molecular interaction of 2,4-diacetylphloroglucinol (DAPG) with human serum albumin (HSA): the spectroscopic, calorimetric and computational investigation, Spectrochim. Acta A Mol. Biomol. Spectrosc. 183 (2017) 90–102.
[19] D. Xiao, L. Zhang, Q. Wang, et al., Investigations of the interactions of peimine and peiminine with human serum albumin by spectroscopic methods and docking studies, J. Lumin. 146 (2014) 218–225.
[20] M. Amiri, K. Jankeje, J.R. Albani, Characterization of human serum albumin forms with pH. Fluorescence lifetime studies, J. Pharm. Biomed. Anal. 51 (2010) 1097–1102.
[21] X. Peng, X. Wang, W. Qi, et al., Deciphering the binding patterns and conformation changes upon the bovine serum albumin–rosmarinic acid complex, Food. Funct. 6 (2015) 2712–2726.
[22] P.L. Kastritis, A.M. Bonvin, On the binding affinity of macromolecular interactions: daring to ask why proteins interact, J. R. Soc. Interface 10 (2013), 20120835, https://doi.org/10.1098/rsif.2012.0835.
[23] F. Poureshghi, P. Ghandforoushan, A. Safarnejad, et al., Interaction of an antiepileptic drug, lamotrigine with human serum albumin (HSA): application of spectroscopic techniques and molecular modeling methods, J. Photochem. Photobiol. B 166 (2017) 187–192.
[24] B. Tang, P. Tang, J. He, et al., Characterization of the binding of a novel antitumor drug ibrutinib with human serum albumin: insights from spectroscopic, calorimetric and docking studies, J. Photochem. Photobiol. B 184 (2018) 18–26.
[25] J. Wang, L. Ma, Y. Zhang, et al., Investigation of the interaction of deltamethrin (DM) with human serum albumin by multi-spectroscopic method, J. Mol. Struct. 1129 (2017) 160–168.
[26] P.D. Ross, S. Subramanian, Thermodynamics of protein association reactions: forces contributing to stability, Biochemistry 20 (1981) 3096–3102.
[27] S.M.S. Abdullah, S. Fatma, G. Rabbani, et al., A spectroscopic and molecular docking approach on the binding of tinzaparin sodium with human serum albumin, J. Mol. Struct. 1127 (2017) 283–288.
[28] G. Sudlow, D.J. Birkett, D.N. Wade, Further characterization of specific drug binding sites on human serum albumin, Mol. Pharmacol. 12 (1976) 1052–1061.
[29] M. Beutler, R. Heintzmann, Förster resonance energy transfer, in: D. Ganten, K. Ruckpaul (Eds.), Encyclopedic Reference of Genomics and Proteomics in Molecular Medicine, vol. 1, Springer, Berlin, Heidelberg, 2006, pp. 594–599.
[30] B.K. Patel, S. Dasmandal, A. Mahapatra, Unraveling the binding of phenolphthalein with serum protein and releasing by β-cyclodextrin, J. Mol. Liq. 244 (2017) 330–339.
[31] M. Pathak, R. Mishra, P.K. Agarwala, et al., Binding of ethyl pyruvate to bovine serum albumin: calorimetric, spectroscopic and molecular docking studies, Thermochim. Acta 633 (2016) 140–148.
[32] Y.J. Hu, Y. Liu, Z.B. Pi, et al., Interaction of cromolyn sodium with human serum albumin: a fluorescence quenching study, Bioorg. Med. Chem. 13 (2005) 6609–6614.

[33] G.F. Shen, T.T. Liu, Q. Wang, et al., Spectroscopic and molecular docking studies of binding interaction of gefitinib, lapatinib and sunitinib with bovine serum albumin (BSA), J. Photochem. Photobiol. B 153 (2015) 380–390.
[34] M.T. Rehman, H. Shamsi, A.U. Khan, Insight into the binding mechanism of imipenem to human serum albumin by spectroscopic and computational approaches, Mol. Pharm. 11 (2014) 1785–1797.
[35] P. Kumar, B. Baidya, S.K. Chaturvedi, et al., DNA binding and nuclease activity of copper (II) complexes of tridentate ligands, Inorg. Chim. Acta 376 (2011) 264–270.
[36] S.K. Chaturvedi, E. Ahmad, J.M. Khan, et al., Elucidating the interaction of limonene with bovine serum albumin: a multi-technique approach, Mol. Biosyst. 11 (2015) 307–316.
[37] X. Liu, Z. Ling, X. Zhou, et al., Comprehensive spectroscopic probing the interaction and conformation impairment of bovine serum albumin (BSA) by herbicide butachlor, J. Photochem. Photobiol. B 162 (2016) 332–339.
[38] A. Ganguly, B.K. Paul, S. Ghosh, et al., Interaction of a potential chloride channel blocker with a model transport protein: a spectroscopic and molecular docking investigation, Phys. Chem. Chem. Phys. 16 (2014) 8465–8475.
[39] H. Yang, Y. Huang, J. He, et al., Interaction of lafutidine in binding to human serum albumin in gastric ulcer therapy: STD-NMR, Water LOGSY-NMR, NMR relaxation times, Tr-NOESY, molecule docking, and spectroscopic studies, Arch. Biochem. Biophys. 606 (2016) 81–89.
[40] M.S. Ali, H.A. Al-Lohedan, Deciphering the interaction of procaine with bovine serum albumin and elucidation of binding site: a multi spectroscopic and molecular docking study, J. Mol. Liq. 236 (2017) 232–240.
[41] M. Roux, B. Perly, F. Djedaïni-Pilard, Self-assemblies of amphiphilic cyclodextrins, Eur. Biophys. J. 36 (2007) 861–867.
[42] T. Loftsson, D. Duchene, Cyclodextrins and their pharmaceutical applications, Int. J. Pharm. 329 (2007) 1–11.
[43] N. Sudha, Y. Sameena, I.V.M.V. Enoch, β-cyclodextrin encapsulates biochanin A and influences its binding to bovine serum albumin: alteration of the binding strength, J. Solut. Chem. 45 (2016) 431–444.
[44] L. Wang, J. Yan, Y. Li, et al., The influence of hydroxypropyl-β-cyclodextrin on the solubility, dissolution, cytotoxicity, and binding of riluzole with human serum albumin, J. Pharm. Biomed. Anal. 117 (2016) 453–463.
[45] Y. Rahman, S. Afrin, M. Tabish, Interaction of pirenzepine with bovine serum albumin and effect of β-cyclodextrin on binding: a biophysical and molecular docking approach, Arch. Biochem. Biophys. 652 (2018) 27–37.
[46] T. Dudev, C. Lim, Competition among metal ions for protein binding sites: determinants of metal ion selectivity in proteins, Chem. Rev. 114 (2014) 538–556.
[47] N. Seedher, P. Agarwal, Effect of metal ions on some pharmacologically relevant interactions involving fluoroquinolone antibiotics, Drug Metab. Drug Interact. 25 (2010) 17–24.
[48] Y. Li, W. He, J. Liu, et al., Binding of the bioactive component jatrorrhizine to human serum albumin, Biochim. Biophys. Acta 1722 (2005) 15–21.
[49] S. Shahraki, M. Saeidifar, F. Shiri, et al., Assessment of the interaction procedure between Pt (IV) prodrug [Pt (5, 50-dmbpy) Cl4 and human serum albumin: combination of spectroscopic and molecular modeling technique, J. Biomol. Struct. Dyn. 35 (2016) 3098–3107.
[50] M. Siddiqi, S. Nusrat, P. Alam, et al., Investigating the site selective binding of busulfan to human serum albumin: biophysical and molecular docking approaches, Int. J. Biol. Macromol. 107 (2018) 1414–1421.
[51] R. Joshi, M. Jadhao, H. Kumar, et al., Is the Sudlow site I of human serum albumin more generous to adopt prospective anti-cancer bioorganic compound than that of bovine: a combined spectroscopic and docking simulation approach, Bioorg. Chem. 75 (2017) 332–346.
[52] D.P. Yeggoni, C. Kuehne, A. Rachamallu, et al., Elucidating the binding interaction of andrographolide with the plasma proteins: biophysical and computational approach, RSC Adv. 7 (2017) 5002–5012.
[53] F. Li, L. Xiu-fen, Z. Qiu-xiang, et al., Characterization of the interactions of human serum albumin (HSA), gatifloxacin, and metronidazole using spectroscopic and electrochemical methods, J. Lumin. 149 (2014) 208–214.
[54] W. Hai, Z. Xiaojuan, P. Wang, et al., Electrochemical site marker competitive method for probing the binding site and binding mode between bovine serum albumin and alizarin red S, Electrochim. Acta 56 (2011) 4181–4187.
[55] Q. Feng, L. Nan-Qiang, J. Yu-Yang, Electrochemical studies of porphyrin interacting with DNA and determination of DNA, Anal. Chim. Acta 344 (1997) 97–104.
[56] E. Biçer, N. Özdemir, Electrochemical and spectroscopic characterization of interaction between antimalarial drug cinchonine and human serum albumin at physiological pH, Russ. J. Electrochem. 50 (2014) 587–593.